Superresolution of Pulsed Multiphoton Raman Transitions

F. S. Cataliotti,* R. Scheunemann, T. W. Hänsch,† and M. Weitz

Max-Planck-Institut für Quantenoptik, Hans-Kopfermann-Straße 1, 85748 Garching, Germany and Sektion Physik der Universität München, Schellingsstraße 4, 80799 München, Germany

(Received 19 September 2000; revised manuscript received 1 June 2001; published 23 August 2001)

We have investigated higher order multiphoton Raman resonances with two pulsed optical frequencies. Multiphoton transfer with up to 50 photons is observed with milliwatts of laser power. We demonstrate that the spectral width of the multiphoton resonances can be far below the Fourier transform linewidth of the driving optical pulses. The functional dependence of the transition linewidth on the number of exchanged photons is found to vary with the pulse shape. Our experiment is performed with laser-cooled rubidium atoms confined in a CO_2-laser optical dipole trap.

DOI: 10.1103/PhysRevLett.87.113601 PACS numbers: 42.50.Hz, 32.80.Wr, 32.80.Pj, 42.65.-k

For an atomic system strongly driven by time-dependent fields multiphoton transitions can occur [1]. It is well known that in such nonlinear processes the spectral width of the atomic response — even in the absence of other broadening mechanisms — does not necessarily reflect the linewidth of the driving ac field. For example, Elliott *et al.* demonstrated that two-photon spectroscopy with a randomly phase-modulated "phase-diffusing" laser field produces a signal that is wider than the Lorentzian spectral profile of the laser beam by a factor of 4 [2]. In general, for N-photon absorption from such a laser field undergoing random phase fluctuations, one expects that the observed width increases by a factor of N^2 [3]. Measured at the laser frequency, the width of the atomic spectrum is then a factor of N larger than the laser beam linewidth.

In this paper, we examine multiphoton Raman transitions using two pulsed optical frequencies and ultracold rubidium atoms confined in a CO_2-laser dipole trap. We find that the spectral width of multiphoton lines for pulsed, transform-limited excitation can be *below* the linewidth (i.e., Fourier width) of the driving optical field. These experimental findings are supported by a simple theoretical model. In our work, multiphoton transfer with up to 50 photons between two stable Zeeman ground state sublevels is achieved with milliwatts of laser power. The multiphoton resonances are observed at subharmonic frequencies of the laser frequency difference required for two-photon Raman transfer. The observed line narrowing of the multiphoton lines for pulsed excitation can be understood by the following argument. Assume that an atom is excited by a nonlinear process proportional to the Nth power of an ac electric field $E(t) = E_0 \cos(\omega t)$. The terms corotating with the atomic oscillator yield a pertubation $V(t) \sim E_0^N e^{-iN\omega t}$. Let us begin by considering the atomic response to a square pulse in time of length T. It is clear that the nonlinear interaction has the same duration in time as the laser pulse, so that its Fourier transform width is just $1/T$, regardless of its carrier frequency being N times higher than that of the laser electric field. For a long lived atomic resonance, the response can be Fourier limited, and the width of the nonlinear resonance observed when tuning the frequency of the field $E(t)$ then is a factor N sharper, i.e., $\Delta\omega = 1/(NT)$. The nature of the line narrowing is such that it should, in principle, allow for an increased resolution in frequency measurements of pulsed radiation, as the spectral width of the multiphoton resonances is below the Fourier limit of the pulse envelope. If a nonsquare pulse is used, the effective length of the nonlinear interaction decreases with N, leading to a certain broadening of the frequency spectrum. Typically, this broadening is only slowly increasing with N, so that a line narrowing of the higher harmonics is also observed for nonsquare pulses. These concepts are readily transferred to the multiphoton Raman case studied in our experiment.

Before proceeding, let us emphasize that multiphoton spectroscopy has a long history in both the optical domain [4] and radiofrequency resonance spectroscopy [5,6]. Examples of optical experiments include the technique of Doppler-free two-photon spectroscopy, multiphoton ionization, Raman spectroscopy, and Doppleron resonances [1,7]. Multiphoton Raman transitions have been observed experimentally, e.g., in collisionally enhanced N-wave mixing in flames [8] and in optical lattices [9]. Despite many applications of pulsed multiphoton spectroscopy, the linewidth of pulsed multiphoton transitions between two bound, long-lived states has not, to our knowledge, been systematically studied in the transform-limited case.

In our experiment, the far-detuned focused radiation near 10.6 μm emitted by a CO_2 laser generates a quasistatic trapping potential for a sample of laser-cooled rubidium atoms [10,11]. The level scheme for multiphoton Raman spectroscopy is shown in Fig. 1a for a transition involving six photons. We investigate the transfer of population between the $m_F = +1$ and $m_F = 0$ Zeeman components of the $F = 1$ hyperfine ground state of the rubidium atom (^{87}Rb), where the degeneracy of the Zeeman sublevels is removed by applying a magnetic bias field δ_{bias}. The Raman transition is driven by two copropagating pulsed optical beams (i.e., oriented in a Doppler-free configuration) with frequencies detuned 23 GHz to the red of the rubidium D2-line near 780 nm. In many respects, the interaction of the bichromatic field with the atom can

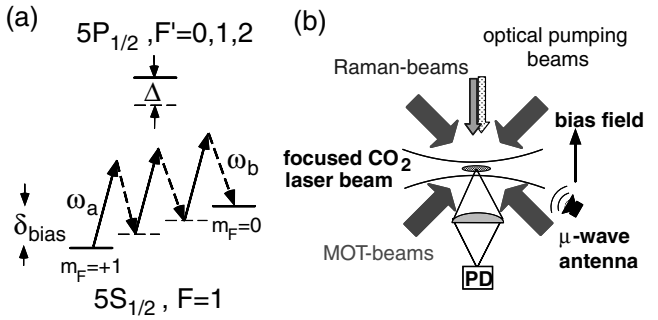

FIG. 1. (a) Scheme of relevant ^{87}Rb atomic levels, showing the energy conservation for a multiphoton Raman transition between two ground state Zeeman sublevels involving three pairs of photons. (b) Schematic of the experimental setup.

be described in terms of an effective interaction containing a term oscillating with the difference of the optical frequencies, which here is in the radio frequency (rf) domain. However, in contrast to rf spectroscopy we expect to observe both odd and even subharmonics of the laser frequency difference for two-photon Raman transfer, i.e., multiphoton Raman transitions can occur when an integer multiple of the frequency difference of the two optical Raman beams $\omega = \omega_a - \omega_b$ coincides with the Zeeman shift δ_{bias} [12,13].

Our setup (Fig. 1b) is similar to that described previously [10,14]. For generation of the dipole trapping potential for atoms, a single-mode CO_2 laser provides radiation near 10.6 μm, which is coupled into the vacuum chamber and focused to a waist of 50 μm. A magneto-optical trap (MOT) superimposed on the focus of the CO_2-laser beam provides cold rubidium atoms, which are loaded into the dipole trap. During the final 5 ms of the MOT loading phase, the repumping laser intensity is extinguished to optically pump the atoms into the lower ($F = 1$) hyperfine ground state and realize a temporal dark MOT. After switching off the near-resonant cooling light and the magnetic quadrupole field for the MOT, the sample of cold atoms is left in the nondissipative dipole potential generated by the CO_2 laser and forms a cigar shaped cloud with an axial width of 200 μm and a radial diameter of 18 μm. We typically confine 10^6 atoms in the dipole trap at a temperature near 80 μK. The expected rate of scattering a photon from the trapping field is suppressed to less than one photon per atom every 10 min. A set of three pairs of Helmholtz coils allows one to control static magnetic fields to roughly 2 mG at the position of the dipole trap. After the cold atomic sample has been stored in the dipole trap, a constant magnetic bias field is applied. The trapped atoms are then optically pumped into the $F = 1$, $m_F = +1$ magnetic ground state sublevel using two additional laser beams tuned to the $F = 1$ to $F' = 0$ and $F = 2$ to $F' = 1$ transition of the rubidium D2-line, respectively.

The Raman beams are generated by splitting light from a Ti:sapphire laser into two and directing each of the beams through an acousto-optic modulator (AOM). The driving frequencies of the AOMs are obtained from two phase-locked function generators. By varying the intensities of these frequencies, arbitrarily shaped optical pulses are produced. The two Raman beams are recombined and overlapped on a polarizing beam splitter, and then sent into the vacuum chamber with orthogonal linear polarizations. The beam axis forms a small angle with respect to the magnetic bias field, such that the atoms experience circular and linear polarization components at both frequencies. The total power of the Raman beams is typically 180 mW with a beam diameter of roughly 4 mm.

The optical beams induce Doppler-free Raman transitions between the Zeeman components $m_F = 1$ and $m_F = 0$ of the $5S_{1/2}$, $F = 1$ ground state. As the laser detuning from the upper state is much larger than the upper state hyperfine splitting, we expect two-photon Raman transfer to occur only between neighboring Zeeman sublevels. We detect the transition by monitoring the population in the final state ($m_F = 0$, $F = 1$) as follows: A microwave π pulse first transfers these atoms to $m_F = 0$, $F = 2$. Subsequently, we irradiate the atomic cloud with light tuned to the $F = 2$ to $F' = 3$ cycling component of the D2 line and detect the resulting fluorescence with a photodiode.

Figure 2 shows typical Raman spectra for different values of the magnetic bias fields. The quoted values for the Zeeman splitting have been calibrated by means of microwave spectroscopy on magnetic field sensitive hyperfine transitions. As expected, we observe a principal Raman resonance (e.g., at 69 kHz in Fig. 2a) when the laser frequency difference ω is near the Zeeman splitting of the sublevels δ_{bias}. Note that the ac Stark effect shifts the position of the Raman resonances towards lower frequencies by a few kHz. In addition, we observe further resonances with decreasing linewidth and amplitude at integer fractions of the principal resonance (e.g., at 34, 23, and 17 kHz in Fig. 2a). We have observed similar spectra when reversing the role of the two Raman beams (i.e., at difference frequencies -17 kHz, -23 kHz, etc.), due to the fact that both optical beams contain linear as well as circular polarization. The subharmonic resonances are attributed to multiphoton Raman transitions between the ground state sublevels involving N pairs of photons, as was shown in Fig. 1a for $N = 3$. Note that this diagram neglects the role of polarization, and shows only the lowest order contribution to the transition occurring at a given laser frequency difference. A transition can occur when a multiple of the frequency difference coincides with the Zeeman shift (neglecting the ac Stark shift), e.g., at $N\omega = \delta_{\text{bias}}$ with N an integer. If we correct for the two-photon ac-Stark shift, the experimental positions of the multiphoton Raman resonances agree with the expected values to within 60 Hz. When the magnetic bias field is decreased, the number of observed subharmonics increases rapidly, as can be seen in Figs. 2b and 2c. This is attributed to a smaller frequency detuning from the intermediate (ground) states for low bias field (see also Fig. 1a), which results in an increased transition probability of especially the higher order

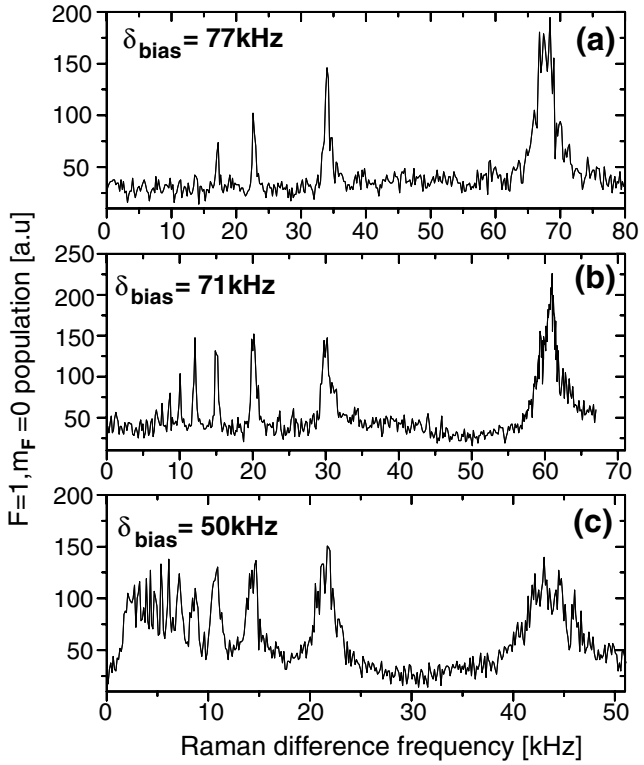

FIG. 2. Multiphoton Raman spectra for different values of applied magnetic bias field δ_{bias}: 50, 71, and 77 kHz (a)–(c). Each data point represents the result of a single run of the experiment. The plots give the population measured in the $F = 1$, $m_F = 0$ ground state hyperfine level after applying a Raman pulse versus the frequency difference between the two Raman beams. The spectra were recorded using 500 μs long Raman pulses with a square pulse envelope.

multiphoton transitions. At very low bias field, the higher order harmonics start to overlap. The number of harmonics observed, e.g., in Fig. 2c can be estimated from the sharp drop in the signal at 2 kHz to be at least $N = 25$.

In order to investigate the narrowing of higher order multiphoton lines in more detail, we have recorded spectra for different pulse durations and pulse shapes. To minimize saturation broadening, we have furthermore varied the optical power level and only analyzed the spectral widths of multiphoton lines with small excitation, where the observed width can be almost totally accounted for by considering the finite interaction time. Figure 3 shows the measured FWHM of Raman subharmonics for a typical set of data recorded with Blackman pulse envelopes [15] of variable length for a constant magnetic bias field ($\delta_{\text{bias}} =$ 50 kHz). The solid line shows the Fourier width of the driving optical pulses. It is clear that the widths of the subharmonic resonances are substantially below that limit. The measured values for the FWHM $\Delta\nu_{1/2}$ of a given subharmonic have been fitted with $\Delta\tau_{1/2}\Delta\nu_{1/2} = c/N^{\alpha}$, where $\Delta\tau_{1/2}$ denotes the FWHM of the optical pulses. The fits are plotted as dashed lines in Fig. 3. This allows one to investigate the dependence of the pulse-duration bandwidth product on the order of the subharmonic N. For the Blackman pulses, we find a $1/N^{0.74(3)}$ dependence.

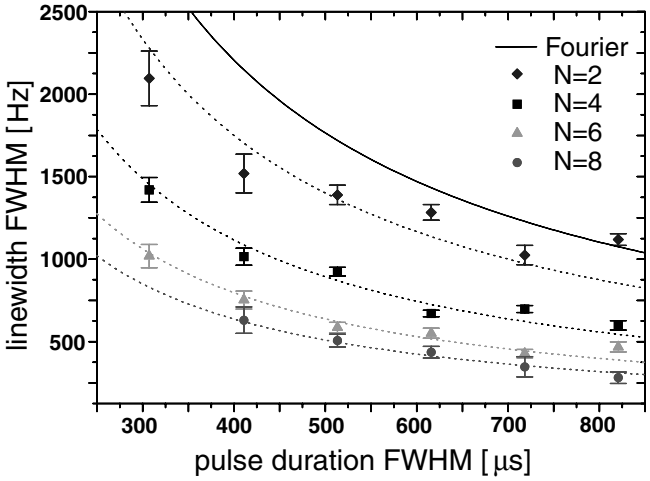

FIG. 3. Measured linewidths $\Delta\nu_{1/2}$ of even Raman subharmonics recorded with Blackman pulse shapes as a function of the pulse duration $\Delta\tau_{1/2}$. The odd subharmonics are also present in the spectra, but are not shown here for clarity. The data points of a given harmonic have been fitted using the function $\Delta\nu_{1/2} \cdot \Delta\tau_{1/2} = c/N^{0.74}$ (dotted lines). The solid line shows the Fourier width of the driving optical pulses.

We have also determined the dependence of the pulse-duration bandwidth product for a square pulse envelope and find a scaling proportional to $1/N^{1.01(3)}$. This is in good agreement with the expected $1/N$ dependence.

The spectral width of the Nth Raman subharmonic, corresponding to a $2N$-photon transition, can be predicted with a simple semiclassical model, where we restrict ourselves to transfers over a single set of intermediate states. After adiabatic elimination of the excited states, we are left with a set of $N + 1$ coupled ground states and consider transfer from the initial state $|g_0\rangle$ over only $N - 1$ intermediate states $|g_m\rangle$ $(0 < m < N)$ to the final state $|g_N\rangle$. We shall use a perturbative approach (i.e., $c_m \ll 1$ for $m > 0$, with $c_m = \langle g_m|\Psi\rangle$) and also neglect ac-Stark shifts. In an interaction picture, where the eigenenergies are factored out of the Hamiltonian, the coupling of levels is described by the set of N differential equations

$$\dot{c}_m = -(i/2)\Omega_{\text{Ram},m}(t)e^{-i\delta_m t}c_{m-1}\,, \tag{1}$$

with $\Omega_{\text{Ram},m}$ as the two-photon Rabi frequencies and $\delta_m = \omega - \omega_{\text{atom}}^{m,m-1}$, where $\omega_{\text{atom}}^{m,m-1}$ denotes the frequency difference between the atomic levels m and $m - 1$. When adiabatically eliminating all intermediate ground states, the set of differential equations reduces to the effective two-level problem

$$\dot{c}_N = -(i/2)\Omega_{\text{eff}}e^{-i(N\omega-\omega_{\text{atom}})t}c_0\,, \tag{2}$$

with the effective $2N$-photon Rabi frequency

$$\Omega_{\text{eff}}(t) = \Omega_{\text{Ram},1}(t)\cdots\Omega_{\text{Ram},N}(t)/(2^{N-1}\delta_1\cdots\delta_{N-1})\,, \tag{3}$$

which is scaling as $(\Omega_{\text{Ram}})^N/\delta_{\text{bias}}^{N-1}$. From this, we derive

$$P_N(\omega)\sim\left|\frac{1}{4}\int_{-\infty}^{\infty}dt'\Omega_{\text{eff}}(t')e^{i(N\omega-\omega_{\text{atom}})t'}\right|^2. \tag{4}$$

for the population in the final state $|g_N\rangle$ after the driving pulse in the limit of small excitations. A line narrowing of the pulsed multiphoton spectra is most easily seen for a square pulse of the driving field, which yields an excitation probability $P_N(\omega) = \Omega_{\text{eff}}^2 \sin[(N\omega - \omega_{\text{atom}})\Delta\tau/2]^2/(N\omega - \omega_{\text{atom}})^2$, where $\Delta\tau$ denotes the pulse length. The FWHM of the Nth multiphoton line is $\Delta\omega = 2\pi/N\Delta\tau$, corresponding to a pulse-duration bandwidth product $\Delta\nu \cdot \Delta\tau = 1/N$, which directly shows the line narrowing of the subharmonics. We wish to stress that the situation considered here differs fundamentally from that described in Refs. [12,13], where a narrowing of multiphoton lines is predicted for cw experiments between levels of finite natural linewidth. For a general pulse shape, Eq. (4) shows that the linewidth of an $2N$-photon transition is $1/N$ times the width of the Fourier transform of the Nth power of the pulse envelope. For example, the pulse-bandwidth product for a multiphoton line driven by a Gaussian pulse of finite length scales as $\sqrt{N} \times 1/N = 1/\sqrt{N}$. The broadening over the $1/N$ scaling expected for square-wave pulses is a secondary effect, caused by nonlinearity of the multiphoton transitions. For Blackman pulse envelopes, a numerical calculation gives an expected $1/N^{0.534(4)}$ dependence of the spectral width on the order of the Raman subharmonic. This is not in good agreement with the experimentally observed value for these pulse envelopes ($1/N^{0.74(3)}$), which we attibute to experimental imperfections in the pulse shaping. Note that the $1/N$ scaling expected for square-wave pulses is very well reproduced by the experiment.

The possibility of achieving multiphoton Raman transfer of high order with moderate optical power levels, as demonstrated in this work, allows one to envision several applications, such as the realization of atom interferometers with large spatial separation between the paths. Coherent momentum transfer can be achieved by performing the Raman transitions in a Doppler-sensitive configuration [16]. Other applications of higher order Raman transitions could include the development of novel techniques for optical scanning supermicroscopy. In the simplest example of tightly focused Raman beams one could take advantage of the well-known benefit that nonlinearities yield an improved spatial resolution. For example, the half-width of the Nth power of the field envelope of a Gaussian waist is a factor $\sqrt{N}$ below the half-width of the field envelope. A similar sharpening effect is also expected in the temporal domain when using pulsed radiation. Our present data already reveal the frequency broadening associated with the temporal sharpening effect. The broader spectrum observed with the smooth Blackman pulses for higher order multiphoton Raman transitions demonstrates the high nonlinearity of these transitions and expresses the possibility of obtaining a sharper "focus" of the effective Rabi frequency in time. Supermicroscopy is, for example, interesting in the context of observing and addressing atoms in single sites of optical lattices, e.g., for quantum computing [14]. An improved spatial resolution also opens further possibilities in quantum lithography [17] (which here might be better phrased as "nonlinear lithography").

The observed line narrowing of the pulsed multiphoton spectra, besides being of fundamental interest, shows that the resolution obtainable, e.g., in spectroscopy of XUV transitions with several visible photons in principle equals that possible with single-photon XUV spectroscopy at a given pulse length (neglecting pulse envelope effects). Certainly, the resolution is not improved over the single-photon result, but the multiphoton technique may have technical benefits due to more accessible laser wavelengths. Finally, the line narrowing of the multiphoton spectra could prove to be useful for measuring or stabilizing the frequency of pulsed optical beams.

To conclude, we have observed subharmonic resonances in pulsed Raman spectra of cold rubidium atoms trapped in a CO_2-laser dipole trap. The resonances are interpreted in terms of higher order multiphoton Raman transitions between two Zeeman ground state sublevels. We have shown that the linewidth of these subharmonics can be substantially smaller than the Fourier width of the driving optical pulses.

This work has been supported in part by the Deutsche Forschungsgemeinschaft and within a European Community science program cooperation.

*Present address: Dipartimento di Fisica, INFM, LENS, Università di Firenze, I–50125 Firenze.

†Also at Dipartimento di Fisica, INFM, LENS, Università di Firenze, I–50125 Firenze.

[1] See, e.g., V. S. Lethokhov and V. P. Chebotayev, *Nonlinear Laser Spectroscopy* (Springer-Verlag, Berlin, 1977).
[2] D. S. Elliott *et al.,* Phys. Rev. Lett. **53**, 439 (1984).
[3] G. S. Agarwal, Phys. Rev. A **1**, 1455 (1970).
[4] W. Kaiser and C. Garrett, Phys. Rev. Lett. **7**, 229 (1961).
[5] J. H. Shirley, Phys. Rev. **138**, B979 (1965).
[6] C. Cohen-Tanoudji, *Cargèse Lectures in Physics,* edited by M. Levy (Gordon and Breach, New York, 1968), Vol. 2; S. Stenholm, J. Phys. B **5**, 878 (1972); **6**, 1097 (1973).
[7] E. Kyrölä and S. Stenholm, Opt. Commun. **22**, 123 (1977), and references therein.
[8] R. Trebino and L. Rahn, Opt. Lett. **12**, 912 (1987).
[9] A. Hemmerich, C. Zimmermann, and T. W. Hänsch, Phys. Rev. Lett. **72**, 625 (1994).
[10] S. Friebel, C. D'Andrea, J. Walz, M. Weitz, and T. W. Hänsch, Phys. Rev. A **57**, R20 (1998).
[11] T. Takekoshi and R. J. Knize, Opt. Lett. **21**, 77 (1996).
[12] G. S. Agarwal, Opt. Lett. **13**, 482 (1988).
[13] H. Wallis, Phys. Rev. A **52**, 1441 (1995).
[14] R. Scheunemann, F. S. Cataliotti, T. W. Hänsch, and M. Weitz, Phys. Rev. A **62**, 051801R (2000).
[15] F. Harris, Proc. IEEE **66**, 51 (1978).
[16] M. Kasevich and S. Chu, Phys. Rev. Lett. **67**, 181 (1991).
[17] A. Boto *et al.,* Phys. Rev. Lett. **85**, 2733 (2000); G. Björk *et al., ibid.* **86**, 4516 (2001).